Noname manuscript No.
(will be inserted by the editor)

Basin of attraction of solutions with pattern formation in Slow-Fast Reaction-Diffusion systems

B. Ambrosio and M.A. Aziz-Alaoui

the date of receipt and acceptance should be inserted later

Abstract This article is devoted to the characterization of the basin of attraction of pattern solutions for some slow-fast Reaction-Diffusion systems with a symmetric property and an underlying oscillatory reaction part. We characterize some subsets of initial conditions that prevent the dynamical system to evolve asymptotically towards these solutions. We also perform numerical simulations that illustrate theoretical results and give rise to symmetric and non-symmetric pattern solutions. We obtain these last solutions by choosing particular random initial conditions.

Keywords Reaction Diffusion Systems · Slow-Fast analysis · Limit-cycles · Pattern Formation · FitzHugh-Nagumo

1 Introduction

Pattern formation arises naturally in widely applications such as chemistry, fluid mechanics, bacteria development, morphogenesis, animals coats designs, visual hallucinations... Among the mathematical models that allows pattern formation, Reaction-diffusion (RD) models are quite relevant. Recall that (RD) systems are partial differential equations with the following form:

$$U_t = F(U) + K\Delta U.$$

We give below some striking biological examples of pattern formation whose behavior has been successfully modeled by Reaction-Diffusion systems. Obviously, this is not exhaustive. The most famous chemical example is certainly the Belousov-Zhabotinsky family of chemical reactions. A mix of a solution of sodium bromate and sulfuric acid and a solution of malonic acid sodium bromure, with a few drops of ferroin, in adequate proportions, will oscillate between red and blue color. If the

B. Ambrosio
Normandy University-Le Havre
E-mail: ambrosio.benjamin@univ-lehavre.fr

same kind of mixture lies on a petri dish, one can observe target or spiral patterns formation. Another patterns such as Turing structures or standing waves have also been observed in Belousov Zhabotinsky chemical reaction types, see [3,10,**?**,**?**,**?**]. Bacteria development also furnishes striking examples of patterns. In this context, RD systems have been successfully used to obtain diffusion-limited aggregation-like, Eden-like, concentric ring-like, disk-like and dense branching morphology-like patterns for the bacteria Bacillus Subtilis development, see [8,9,11]. Dictyostellium Discodeum amoeba, in condition of starvation also exhibits spectacular patterns that have been modelled by reaction diffusion systems, see [7,**?**]. In physiological context spiral or target patterns can be found in excitable or oscillatory cells such as cardiac tissue or brain, see [12]. A well known example of pattern formation in physiological context is the appearance of visual patterns related to drug induced hallucinations. A mathematical modeling approach has been developed for that, see [5,4] and references therein cited. From a mathematical point of view pattern formation in reaction diffusion systems has attracted numerous researchers. The first mathematical well-known analysis came with the seminal work of Turing[15], in which a two component system of reaction diffusion is proposed to explain the morphogenesis. Mathematically, the phenomena known as Turing mechanism occurs when the diffusion-less system possess a stable stationary solution and the diffusion term turn the stationary point unstable, leading to stable patterns solutions. The mathematical technique, largely used, consists then on exhibiting sufficient conditions in order to obtain positive eigenvalues for the jacobian at the steady state, see for example [12]. In the same idea, one can get stable patterns if the underlying ODE system possesses a bistability property. When the underlying ODE is either excitable or oscillatory wave propagation may occur that eventually results on pattern formation. In the context of excitable media, wave propagation results from the diffusion term: the excitation wave may propagate trough excitation of neighbors. Note that this idea already appears in the works of [**?**,**?**]. In case of oscillatory media the wave propagation results from a shift in oscillations regarding to the space location. It is important to note that symmetry plays a key role in pattern formation. This idea was already found in [15]. Since this pioneering work, an important and interesting theory has been developed to study the role of symmetry in dynamical systems, see [6]. Among all these cases where RD systems may lead to pattern formation, we will focus in the following one: RD-systems with two components and a symmetric oscillatory reaction term. More precisely, we will focus on the characterization of the basin of attraction of special patterns for reaction-diffusion systems whose underlying ODE reaction system has the following property: the unique fixed point is the origin and all solution initiating from a value distinct from the origin evolves asymptotically around a limit cycle. We will also assume that, the ODE has a symmetry property, for example if $U(t)$ is a solution, $-U(t)$ also is a solution. A typical ODE system of this kind is given by the following $FitzHugh-Nagumo$ system:

$$\begin{cases} \varepsilon u_t = f(u) - v \\ v_t = u - \delta v \end{cases} \tag{1}$$

where $f(u) = -u^3 + 3u$, ε is small parameter, and δ not to large. Let us recall that the FitzHugh-Nagumo system is a simplification of the Hodgkin-Huxley model

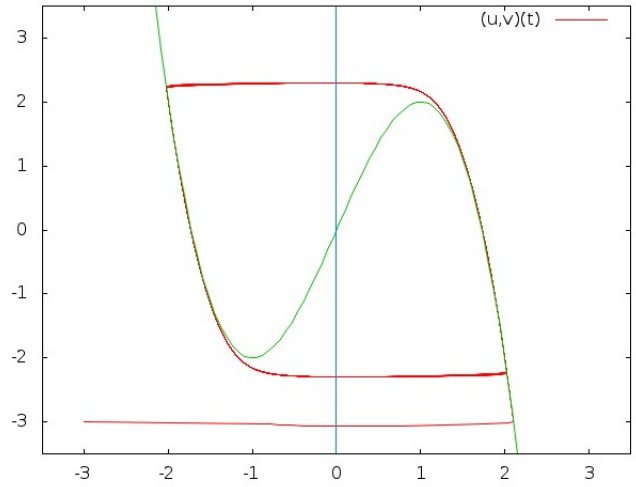

that can exhibit oscillatory or excitable behavior. In this system, the variable u represents the cellular electric potential while the variable v is a recovery variable. For the version studied here, it is oscillatory. Indeed, the figure 1 illustrates the asymptotic behavior of system (1).

Throughout this paper we will mainly deal with the following reaction-diffusion system:

$$\begin{cases} \varepsilon u_t = f(u) - v + d_u \Delta u \\ v_t = u - \delta v + d_v \Delta v \end{cases} \tag{2}$$

whith $f(u) = -u^3 + 3u$, ε small, δ not to large, $d_u > 0, d_v \geq 0$ and Neumann Boundary conditions (NBC) but theoretical results remain valid for systems with analog properties. We are interested in the characterization of the basin of attractions of (2). More precisely, we know that the system generates a semi-group and posseses a global attractor in $L^2(\Omega) \times L^2(\Omega)$ and a bound in $L^\infty(\Omega) \times L^\infty(\Omega)$, see for example [AMbrosio, Marion, Phan. ..]. Note that other frameworks are possible such as classical and holder function spaces, see [13]. Amoung the elements of the attractor, some are well-known: the elements constant in space and belonging to the attractor of (1). In other words, if we choose initial conditions of (2), $(u_0(x), v_0(x))$ constant in space, and if (u,v) is a solution of (2), then for all fixed $x \in \Omega$, $(u(x,t), v(x,t))$ is a solution of (1) which evolves toward the limit-cycle as soon as $(u_0(x), v_0(x)) \neq (0,0)$. Numerical simulations show that almost of initial conditions will evolve asymptotically toward this solution. In the case where,

$$\lambda d_u > 3, \tag{3}$$

where λ is the smallest non-zero eigenvalue of $-\Delta$ with *NBC*, all the solutions evolve asymptotically towards space homogeneous solutions, that is, towards the limit cycle

of (1) or towards $(0,0)$, see [1,2]. A question naturally arises: when (3) is not fulfilled, are we able to characterize the initial conditions that will not evolve toward homogeneous space solutions? The aim of this article is to discuss this question and furnish some theoretical and numerical elements of response. Indeed, the article is divided in five parts as follows. After the current introducing part, we give some crucial elements giving some insights on the stability of the space-homogeneous periodic solution of (2), in the second part. In the third part, we give sufficient conditions that implies an asymptotic non-homogeneous space behavior. This means that we will characterize some elements of the basin of attractions of non-homogeneous-space elements of the attractor. For this we use the symmetry of the equation (2): if (u,v) is a solution, also $-(u,v)$ is. Also we will consider symmetric domains. This means that we will be able to choose appropriate initial conditions, leading to null integrals $\int_\Omega u dx$ and $\int_\Omega v dx$. Therefore, this prevents the solution to evolve toward the limit cycle solution of (1). In the forth part, we perform numerical simulations. We illustrate some applications of the theoretical results of the third part and also exhibit numerically another initial conditions that will evolve asymptotically to non-homogeneous space solutions. For this we will choose initial conditions distributed along stochastic laws. We will show numerical evidence that choosing initial conditions with stochastic laws of null expectancy leads to asymptotically non-homogeneous space solutions but woth less symmetry. The conclusion is left to the last part. We denote by $(\tilde{u},\tilde{v})$ the periodic solution of (1).

2 Stability of the homogeneous solution $(\tilde{u},\tilde{v})$ for (2)

In this part we give two propositions giving insights on the stability of $(\tilde{u},\tilde{v})$ using slow-fast analysis. The rigorous proof of this stability, however, present some technical subtelties and it is left for a forthcoming paper. We rewrite (2) around $(\tilde{u},\tilde{v})$, this gives:

$$\begin{cases} \varepsilon u_t = f'(\tilde{u})u + \frac{f''(\tilde{u})}{2}u^2 - u^3 - v + d_u \Delta u \\ v_t = u - \delta v + d_v \Delta v \end{cases} \tag{4}$$

The layer system writes:

$$\begin{cases} u_t = f'(\tilde{u}(0))u + \frac{f''(\tilde{u}(0))}{2}u^2 - u^3 - v + d_u \Delta u \\ v_t = 0 \end{cases} \tag{5}$$

while the reduced system writes:

$$\begin{cases} 0 = f'(\tilde{u}(t))u + \frac{f''(\tilde{u}(t))}{2}u^2 - u^3 - v + d_u \Delta u \\ v_t = u - \delta v + d_v \Delta v \end{cases} \tag{6}$$

We split the proof into two lemmas. We start with the first one which gives the asymptotical behavior of the layer system. Let us consider the following equation:

$$u_t = g(u) - v + d_u \Delta u. \tag{7}$$

We have:

Proposition 1 *Let $X = C^0(\bar{\Omega})$ endowed with the norm $||f|| = \sup_{x\in\bar{\Omega}} |f(x)|$. We assume that $g \in C^1()$ is such that $g(0) = 0$ and $g'(0) < 0$, then for $||v||$ small enough and $u_0 \in X \cap C^2(\bar{\Omega})$ such that $||u_0||$ small enough the solution u of (7) evolves towards the (locally) unique stationary solution of (7) in X.*

Proof The proof basically relies on maximum principles. Note that because of Neumann boundary conditions maximum or minimums cannot occur on boundaries, see [**?**]. We give here a direct proof. Since $g'(0) < 0$, g is locally decreasing in a closed interval I containing 0, for $||v||$ small enough, we can find u_0 and two constant values a and $b \in I$ such that $a < u_0(x) < b$, with:

$$g(a) - v(x) > 0,$$

$$g(b) - v(x) < 0,$$

and $g'(x) < 0$ in $[a,b]$. This means that a is sub-solution and b an upper-solution of (7), see for example [14]. Let us denote by $u_a(x,t)$ the solution of (7) with $u_a(x,0) = a$, then for all $t > 0$, $a < u_a < b$. Indeed, if u_a reaches b for the first time, equation (7) leads to $0 \leq u_{at} = g(b) - v + d_u \Delta u_a < 0$, which is a contradiction. Analogously, since $u_{at}(x,0) = g(a) - v > 0$, u_a is greater than a for t small enough. Therefore, if u_a reaches a for the first time, we have $0 \geq u_{at} = g(a) - v + d_u \Delta u_a > 0$ which is a contradiction. Therefore for all $t > 0$, $a < u_a < b$. Note that this result remains valid for any solution such that $a \leq u_0 \leq b$, but we focus for the moment on the solution with $u_0 = a$. We set $w = u_{at}$. Then

$$w_t = g'(u_a)w + d_u \Delta w, \tag{8}$$

and

$$w_0 = g(a) - v > 0.$$

By analog arguments we can prove that $w \geq 0$ (consider the first time such that w reaches a value $w_- < 0$). We will prove that in fact $w > 0$ and we will give an uniform bound, depending only on time. Let $l_m = \min_{x\in[a,b]} g'(x)$ and $l_M = \max_{x\in[a,b]} g'(x)$. We have $l_m < l_M < 0$. Let $\underline{w}$ the solution of $w_t = l_m w$ with $\underline{w}_0 = \inf_{x\in[a,b]} w_0$. Then we have

$$w_t \geq l_m w + d_u \Delta w,$$

and therefore,

$$(w - \underline{w})_t \geq l_m(w - \underline{w}) + d_u \Delta (w - \underline{w}).$$

Hence $w - \underline{w} \geq 0$, which means:

$$u_{at} \geq \underline{w}_0 e^{l_m t}.$$

With same arguments, we show that $u_{at} = w$ converges uniformly toward 0. Let u_b the solution of (7) with $u(0) = b$, u converges uniformly to a continuous function. By analog comparison arguments we show that $u_b - u_a$ converges uniformly toward 0. Indeed, let $h = u_b - u_a$. We have:

$$h_t = g'(\theta)h + d_u \Delta h$$

with $\theta(x,t) \in]a,b[$. We have $h \geq 0$. Let $\bar{h}$ solution of $h_t = l_M h$ with $\bar{h}_0 = \max_{x\in\bar{\Omega}}(u_b - u_a)$ and $\underline{h}$ solution of $h_t = l_m h$ with $\underline{h}_0 = \min_{x\in\bar{\Omega}}(u_b - u_a)$. Then,

$$h_t \leq l_M h + d_u \Delta h,$$

and

$$(\bar{h} - h_t) \leq l_M(\bar{h} - h) + d_u \Delta(\bar{h} - h).$$

Also,

$$(h - \underline{h})_t \geq l_m(h - \underline{h}) + d_u \Delta(h - \underline{h}).$$

Therefore,

$$\underline{h}_0 e^{l_m t} \leq h \leq \bar{h}_0 e^{l_M t}.$$

It follows that h converges uniformly toward 0. Therefore u_a and u_b converge uniformly towards a function, let's say u^*. Next, we show that u^* is a solution of $g(b) - v + d_u \Delta u = 0$. As u_{at} converges uniformly toward 0, we have

$$g(u^*) - v + d_u \Delta u^* = 0. \tag{9}$$

Also, as u_{at} and $g(u_a)$ converges uniformly, this implies that Δu_a converges uniformly. Same arguments are valid to show, that any solution of (7), starting with $u_0 \in [a,b]$, will converge uniformly toward a solution of (9). For the unicity, let u_1 and u_2 two solutions of the stationary equation belonging to the interval $[a,b]$. Then:

$$g'(\theta)(u_1 - u_2) + d_u \Delta(u_1 - u_2) = 0.$$

By integrating by parts or by a maximum principle this implies that $u_1 - u_2 = 0$.

The proposition 2 shows that the reduced system decreases exponentially in norm L^2 as long as $(\tilde{u},\tilde{v})$ and (u,v) remain in the attractive parts of the cubic. We set $g(t,u) = f'(\tilde{u}(t))u + \frac{f''(\tilde{u}(t))}{2}u^2 - u^3 = 3(1-\bar{u}^2)u - 3\bar{u}u^2 - u3$. Let $a(t) = -\bar{u} - 1$ and $b(t) = -\bar{u} + 1$. Let $v(x,t)$ a solution of (6).

Proposition 2 *Let $I = [t_0,t_1]$ such for all $t \in I$ that $f'(\bar{u}(t)) < -1$ (resp $f'(\bar{u}(t)) > 1$) and that $v(x,t) \in [g(t,a(t)),+\infty[$ (resp $]-\infty, g(t,b(t))]$). Then for all $t \in [t_0,t_1]$, we have*

$$\int_\Omega v^2(x,t)dx \leq e^{-\delta(t-t_0)} \int_\Omega v^2(x,0)dx$$

Proof We multiply the second equation of (6) by and integrate over Ω, we obtain:

$$\frac{d}{dt}\int_\Omega v^2(x,t)dx = 2(\int_\Omega uvdx - \delta\int_\Omega v^2 dx - \int_\Omega v\Delta v dx).$$

By multiplying now the first equation of (6) and integrating over Ω, we have

$$\int_\Omega uvdx = \int_\Omega g(t,u)udx + \int_\Omega u d_u \Delta u dx.$$

The assumptions of the proposition imply that $\int_\Omega g(t,u)udx \leq 0$ for $t \in [t_0,t_1]$. Therefore, using green formula, we obtain:

$$\frac{d}{dt}\int_\Omega v^2(x,t)dx \leq -2\delta\int_\Omega v^2 dx).$$

Then the result follows from multiplying by $e^{2\delta t}$ and integrating.

3 A condition for evolution toward patterns

Let us denote $(\bar{u},\bar{v})$ the limit-cycle of (1). The following theorem exhibits initial conditions that prevent the solution of (2) to be asymptotically homogeneous and evolve to $(\bar{u},\bar{v})$.

Theorem 1 *Suppose that we can divide the domain into a partition* $\Omega = (\cup_{i\in\{1,...,l\}})\cup(\cup_{i\in\{1,...,l\}}V_i)$ *such that for* $i \in \{1,...,l\}$ *there exists a diffeomorphism* ϕ *from* U_i *to* V_i *with* $|\det J_{\phi_i}| = 1$*, where* J *is the jacobian of* ϕ *and initial conditions such that for all* $x \in \cup_{i\in\{1,...,l\}}U_i)$ *and for all* $t \in^+$*,* $(u_i(\phi_i(x),t),v_i(\phi_i(x),t)) = -(u_i(x,t),v_i(x,t))$ *then the solution of* (2) *can not evolve asymptotically toward* $(\bar{u},\bar{v})$*.*

Proof If the hypothesis of theorem 1 are verified then, for all $t > 0$:

$$\begin{aligned}\int_\Omega u(x,t)dx = & \sum_{i=1}^{l}\int_{U_i}u(x,t)dx+\sum_{i=1}^{l}\int_{V_i}u(x,t)dx\\ = & \sum_{i=1}^{l}\int_{U_i}u(x,t)dx+\sum_{i=1}^{l}\int_{U_i}u(\phi_i(x),t)|\det J_{\phi_i}|dx\\ = & \sum_{i=1}^{l}\int_{U_i}u(x,t)dx-\sum_{i=1}^{l}\int_{U_i}u(x,t)dx\\ = & 0\end{aligned}$$

The result is valid for $\int_\Omega v(x,t)dx$. And we know that for all t:

$$\int_\Omega(\bar{u}(t),\bar{v}(t) \neq (0,0).$$

The two following corollaries give examples of situations where theorem 1 apply.

Corollary 1 *Suppose that the domain* Ω *has* $(0,0)$ *as symmetry center and that for all* $x = (x_1,x_2) \in \Omega(u_0,v_0)(x) = -(u_0,v_0)(-x)$ *then for all* $t > 0$ *and for all* $x \in \Omega,(u,v)(x,t) = -(u,v)(-x,t)(resp(u,v)(x,t) = -(u,v)(-x_1,x_2,t),(u,v)(x,t) = -(u,v)(x_1,-x_2,t))$*. Then the solution of* (2) *can not be asymptotically homogeneous and evolve asymptotically toward* $(\bar{u},\bar{v})$*.*

Proof This follows from symmetry, and the property that $(f(-u)+v,-u+\delta v) = -(f(u)-v,u-\delta v)$.

Corollary 2 *Suppose that the domain* Ω *has* $(x_1,0)$ *as axis symmetry and that for all* $x = (x_1,x_2) \in \Omega$ $(u_0,v_0)(x_1,x_2)) = -(u_0,v_0)(x_1,-x_2))$ *then for all* $t > 0$ *and for all* $x \in \Omega$*,* $(u,v)(x,t) = -(u,v)(x_1,-x_2,t))$*. It follows that the solution of* (2) *can not be asymptotically homogeneous and evolve asymptotically toward* $(\bar{u},\bar{v})$*.*

Proof This follows from symmetry, and the property that $(f(-u)+v = \Delta(-u),-u+\delta v) = -(f(u)-v+\Delta u,u-\delta v)$.

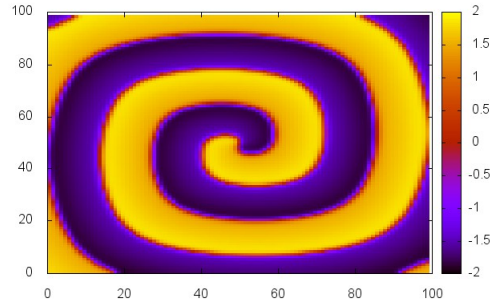

Fig. 1 This figure shows the asymptotical evolution of a solution of (2). More precisely, it represents the isovalues of $u(x_1,x_2,t)$ for time $t = 190$. It is obtained by choosing $(u_0(x),v_0(x) = (1,0)$ on the quarter left-up square, $(u_0(x),v_0(x) = (0,1)$ on the quarter right-up square, quarter left-up square, $(u_0(x),v_0(x) = (0,-1)$ on the quarter left-down square and $(u_0(x),v_0(x) = (-1,0)$ on the quarter right-down square. This illustrates an asymptotic non homogeneous space behavior of a spiral type. It is an application of the corollary 1

4 Numerical simulations

In this section we present some numerical simulations of (2) leading to pattern formation. We use a $C++$ program with aa difference finite scheme in space and RK4 in time. We choose a time step $dt = 0.01$ on the intervall $[0,200]$ and a space step $h = 1$ on the square domain $[0,100] \times [0,100]$. Also we choose $d_u = 1, d_v = 0, \varepsilon = 0.1, \delta = 0.2$. Numerical simulations in figures above.

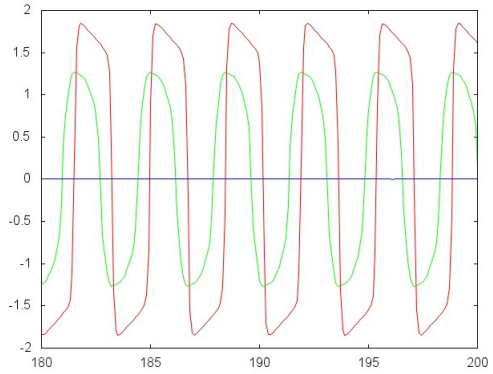

Fig. 2 This figure shows the asymptotic evolution of a solution of (2) at some space points. Indeed, the green line represents $u(x_1,x_2,t)$ for $(x_1,x_2) = (50,50,t)$, for time $t \in [180,200]$. The red line represents $u(x_1,x_2,t)$ for $(x_1,x_2) = (50,100,t)$, for time $t \in [180,200]$. Finally, the blue line represents $\int_\Omega u(x,t)dx$, which is zero as predicted by the theory. It is obtained by choosing the same initial conditions as in figure 4. This illustrates an asymptotic non homogeneous space behavior. For each $x \in \Omega$ the trajectory evolves asymptotically around limit cycles of same period, the patterns observed result from a phase shift.

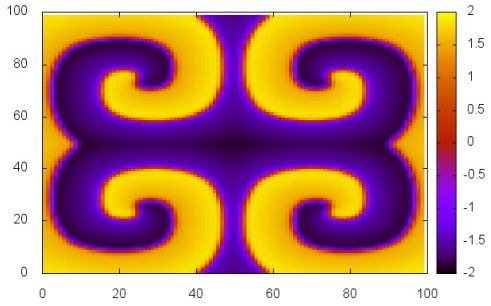

Fig. 3 This figure shows the asymptotic evolution of a solution of (2). It represents $u(x_1,x_2,t)$ for time $t = 190$. It is obtained by reproducing for times the initial conditions of figure 4 by axial symmetry. More precisely, we reproduce the initial conditions of figure 4 in the upper-left quarter square. Then, we operate an axial symmetry of axis $(x_1,0)$ to obtain the initial conditions on the quarter down-left square, and an axial symmetry of axis $(0,x_2)$ to obtain the initial conditions on the upper-right quarter square. Finally, we choose initial conditions on the down-right quarter by central symmetry of the upper-left or equivalently by axial symmetry of the upper-right or down-left quarter square. Then, we obtain four spirals. By the way, we can show by symmetry that choosing such initial conditions, implies that the solution on the upper-left quarter verify (2) with NBC. Then, it comes from symmetry that we obtain four times the same patterns. We can repeat this procedure as many times as needed.

References

1. Ambrosio, B., Aziz-Alaoui, M.: Synchronization and control of a network of coupled reaction-diffusion systems of generalized fitzhugh-nagumo type. ESAIM:Proceedings **39** (2013)
2. Conway, E., Hoff, D., Smoller, J.: Large-time behaviour of solutions of systems of non linear reaction-diffusion equations. SIAM J. Appl. Math **35**, 1–16 (1978)

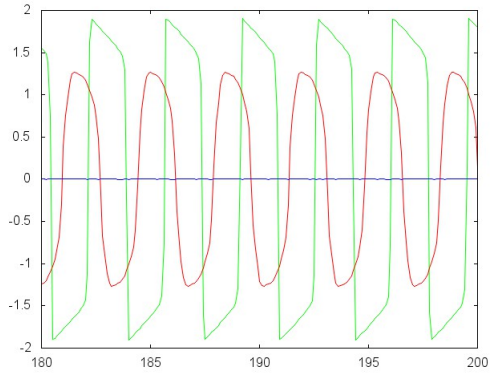

Fig. 4 This figure shows the asymptotic evolution of a solution of (2) at some space points. Indeed, the green line represents $u(x_1,x_2,t)$ for $(x_1,x_2) = (50,50,t)$, for time $t \in [180,200]$. The red line represents $u(x_1,x_2,t)$ for $(x_1,x_2) = (50,100,t)$, for time $t \in [180,200]$. Finally, the blue line represents $\int_\Omega u(x,t)dx$, for time $t \in [180,200]$, which is zero as predicted by the theory. It is obtained by choosing the same initial conditions as in figure 4. This illustrates an asymptotic non homogeneous space behavior. For each $x \in \Omega$ the trajectory evolves asymptotically around limit cycles of same period, the patterns observed result from a phase shift.

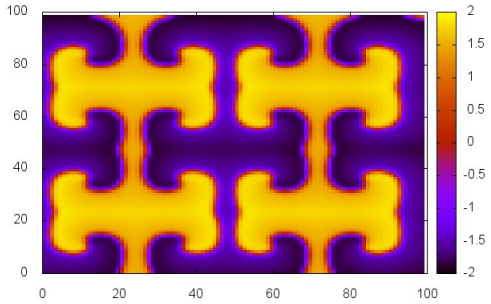

Fig. 5 This figure shows the asymptotic evolution of a solution of (2). It represents $u(x_1,x_2,t)$ for time $t = 190$. It is obtained by operating two times the procedure described in figure 4. We obtain sixteen spirals. However, we have to notice that in this case, because of our discretization, we don't have a perfect symmetry for initial conditions. Indeed, some domains are slighty bigger than other, for example the left-down corner in which we take a constant initial contain 13×13 (because $13 = 100/8+1$) points while the opposite region where we choose symmetric value contains 12×12 points. Therefore, the symmetry is not perfectly verified.

3. Epstein, I.R., Showalter, K.: Nonlinear chemical dynamics: Oscillations, patterns, and chaos. J. Phys. Chem. **100**, 13,132–13,147 (1996)
4. Ermentrout, G., Cowan, J.: A mathematical theory of visual hallucilations patterns. Biol. Cybernetics **34**, 137150 (1979)
5. Golubitsky, M., Shiau, L.J., Torok, A.: Symmetry and pattern formation on the visual cortex. Dynamics and Bifurcation of Patterns in Dissipative Systems. Series on Nonlinear Science **12**, 3–19 (2004)
6. Golubitsky, M., Stewart, I.: The Symmetry Perspective. Birkhauser (2002)
7. Halloy, J., Lauzeral, J., Goldbeter, A.: Modelling oscillations and waves of camp in dictyostelium discoideum cells. Biophysical chemistry **79**, 9–19 (1998)

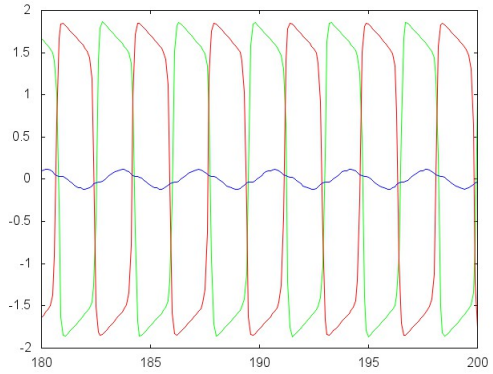

Fig. 6 This figure shows the asymptotic evolution of a solution of (2) at some space points. Indeed, the green line represents $u(x_1,x_2,t)$ for $(x_1,x_2) = (50,50,t)$, for time $t \in [180,200]$. The red line represents $u(x_1,x_2,t)$ for $(x_1,x_2) = (50,100,t)$, for time $t \in [180,200]$. Finally, the blue line represents $\int_\Omega u(x,t)dx$, for time $t \in [180,200]$. It is obtained by choosing the same initial conditions as in figure 4. This illustrates an asymptotic non homogeneous space behavior. For each $x \in \Omega$ the trajectory evolves asymptotically around limit cycles of same period, the patterns observed result from a phase shift. Here the value of $\int_\Omega u(x,t)dx$ is non zero, but rather periodic. Here the theoretical results of the previous section do not apply as our initial solutions do not verify the symmetric conditions.

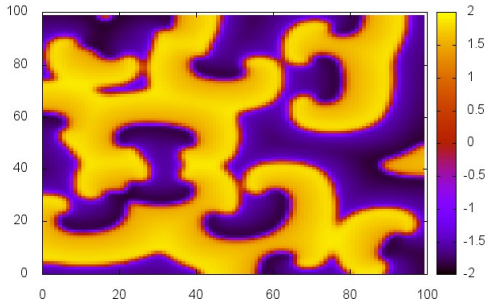

Fig. 7 This figure shows the asymptotic evolution of a solution of (2). More precisely, it represents $u(x_1,x_2,t)$ for time $t = 190$. It is obtained by choosing for all $x \in \Omega$, $(u_0(x),v_0(x))$ as a realization of an uniform stochastic variable on $[-1,1]$. This illustrates an asymptotic non homogeneous space behavior.

8. Lacasta, A., Cantalapiedra, I., Auguet, C., Peñaranda, A., Ramírez-Piscina, L.: Modeling of spatiotemporal patterns in bacterial colonies. Phys. Rev. E Stat. Phys. Plasmas Fluids Relat. Interdiscip. **Topics 59**, 7036 (1999)
9. Matsushita, M., Wakita, J., Itoh, H., Rafols, I., Matsuyama, T., Sakaguchi, H., Mimura, M.: Interface growth and pattern formation in bacterial colonies. Physica A **249**, 517–524 (1998)
10. Mikhailov, A., Showalter, K.: Control of waves, patterns and turbulence in chemical systems. Physics. Reports. **425**, 79–194 (2006)
11. Mimura, M., Sakaguchib, H., Matsushita, M.: Reaction-diffusion modelling of bacterial colony patterns. Physica A **282**, 283–303 (2000)
12. Murray, J.: Mathematical Biology. Springer (2010)
13. Rothe, F.: Global Solutions of Reaction-Diffusion Systems. Springer (1984)
14. Smoller, J.: Shock Waves and Reaction Diffusion. Springer-Verlag (1994)

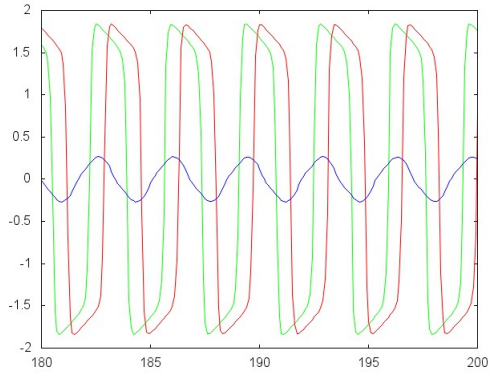

Fig. 8 This figure shows the asymptotic evolution of a solution of (2) at some space points. Indeed, the green line represents $u(x_1,x_2,t)$ for $(x_1,x_2) = (50,50,t)$, for time $t \in [180,200]$. The red line represents $u(x_1,x_2,t)$ for $(x_1,x_2) = (50,100,t)$, for time $t \in [180,200]$. Finally, the blue line represents $\int_\Omega u(x,t)dx$, for time $t \in [180,200]$. As previously the figure is obtained by choosing for all $x \in \Omega$, $(u_0(x),v_0(x))$ as a realization of an uniform stochastic variable on $[-1,1]$. This illustrates an asymptotic non homogeneous space behavior. For each $x \in \Omega$ the trajectory evolves asymptotically around the same limit cycle, the patterns observed result from a phase shift. We can see that the value of $\int_\Omega u(x,t)dx$ oscillate between approximatively -0.2 and 0.2 as it was the case for the solution with sixteen spirals. In this case also the zero-integral condition with symmetry is not verified for initial conditions.

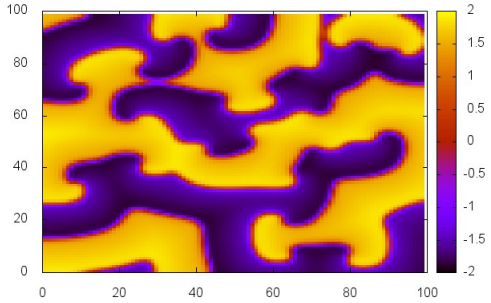

Fig. 9 This figure shows the asymptotic evolution of a solution of (2). More precisely, it represents $u(x_1,x_2,t)$ for time $t = 190$. It is obtained by choosing for all $x \in \Omega$, $(u_0(x),v_0(x))$ as a realization of a stochastic variable following the law $\mathcal{N}(0,1)$. This illustrates an asymptotic non homogeneous space behavior as it was the case for stochastic uniform initial conditions.

15. Turing, A.M.: The chemical basis of morphogenesis. Phil. Trans. R. Soc. B

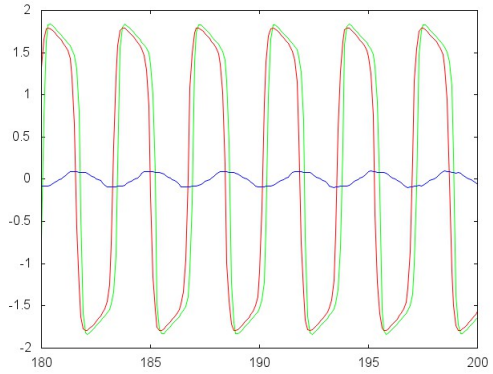

Fig. 10 This figure shows the asymptotic evolution of a solution of (2) at some space points. Indeed, the green line represents $u(x_1,x_2,t)$ for $(x_1,x_2) = (50,50,t)$, for time $t \in [180,200]$. The red line represents $u(x_1,x_2,t)$ for $(x_1,x_2) = (50,100,t)$, for time $t \in [180,200]$. Finally, the blue line represents $\int_\Omega u(x,t)dx$, for time $t \in [180,200]$. As previously the figure is obtained by choosing for all $x \in \Omega$, $(u_0(x),v_0(x))$ as a realization of a stochastic variable following the law $\mathcal{N}(0,1)$. This illustrates an asymptotic non homogeneous space behavior. For each $x \in \Omega$ the trajectory evolves asymptotically around the same limit cycle, the patterns observed result from a phase shift.As previously the value of $\int_\Omega u(x,t)dx$ oscillate between approximately -0.2 and 0.2.